Chapter 4

Convex and concave collector designs of self-driven SAH

Conventional natural convection flat plate solar air heater (SAH) suffers from low heat transfer characteristics. Putting extended surfaces in the air flow channel to augment thermal performance actually hinders the buoyancy driven flow, and thereby reducing the hydraulic performance due to high frictional losses. The objective of the present study is to enhance thermo-hydraulic performance by incorporating convex and concave flow channel with chimney effect. The curved SAH has been investigated using an experimentally validated computational fluid dynamic model for different curvature angles in the range of $25^\circ - 50^\circ$. *The results show significant increase in Nusselt number per unit pressure drop (NuP), heat transfer enhancement factor, temperature enhancement ratio and effectiveness, in comparison to conventional flat SAH. The convex and concave designs are respectively 4.3% and 3.1% thermally, and 7% and 6% by NuP, higher than conventional flat natural convection SAH. Two different independent correlations derived for Nusselt number for different geometries were found to be in excellent agreement with the data. The designs and data presented in the study would help scientific community and solar based industries in developing efficient natural convection SAH.*

4.1 Introduction

The energy needs for operating devices to perform different applications have been increasing all around the world. Solar energy is used in various applications such as electricity production [124], water purification [128], air and water heating [144, 127]. Solar air heaters (SAH) are becoming preferred choice for energy conversion for low to medium range temperatures such as space heating or crop drying applications. The solar air heaters based on the forced convection consumes significant power, and hence the cost associated for its operation. The solar air heaters operate on the principle of natural convection are independent of power requirements, but have been suffering from low thermal efficiency. Many literature's report diverse techniques to increase thermal performance of natural convection SAH by integration of ribs of various shape [53, 68, 119] on the absorber surface. It is an established fluid dynamics fact that any form of intrusion in the flow passage increases friction losses [68, 119]. Friction losses or pressure drop P is directly proportional to the magnitude of average velocity V of the flow i.e. $P \sim kV^2$ where k is a constant for a specific system. Higher velocity results in higher hydraulic losses. In case of solar air heaters that are primarily dependent on external sources of power to drive the flow such as fan or blower, this additional pressure drop due to internal fins or ribs may not pose a serious concern as the primary aim is the enhancement of heat transfer coefficient [119, 145]. However, in case of natural convection solar air heaters, the primary source that drives the flow is buoyancy force.

Low air flow velocities in buoyancy driven solar air heaters offers serious challenges in increasing the systems rate of heat transfer, when internal obstructions in the form of fins are present. Previous investigations have primarily focused on thermal performance enhancement at the expense of hydraulic performance. For example, flat natural convection SAH has been investigated with various shapes of extended surfaces along the flow channel such as offset rectangular [125], conical [10, 3], v and w- shape turbulators [90, 153, 140], arc shape obstacles [143, 108]; square ribs [144], taper shape obstacles [56], truncated ribs [135], twisted shape inserts [93],

C-shape ribs [47] and wavy fins [48].

Apart from decreasing the air mass flow rate due to frictional losses, these ribs increase additional fabrication and maintenance cost. Hence, primary aim in designing the natural convection solar air heaters is dual i.e. increase thermal (enhance heat transfer coefficient) and hydraulic (negligible friction losses) performance. However, these requirements are generally conflicting in nature. Higher thermal performance comes at the expense of higher hydraulic losses as it requires putting extended surfaces on the absorber plate to enhance heat transfer rates [133, 73].

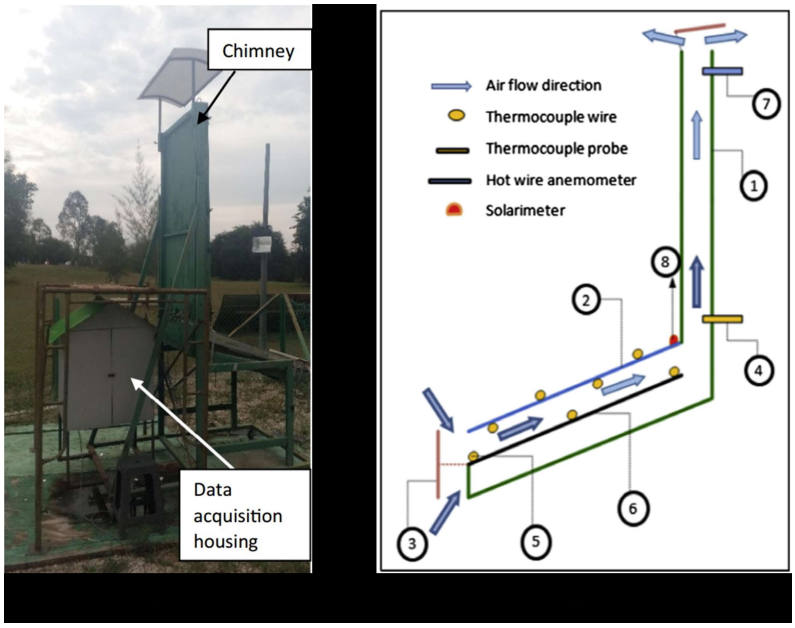

Figure 4.1: Experimental set up of a conventional flat plate natural convection solar air heater (Gilani et al., 2017): (a) chimney, solar air heater and data collection unit, (b) side view showing the flow direction and location of measuring instruments (1- chimney, 2- double glaze glass top cover, 3- wind protector, 4- probe thermocouple, 5- wire thermocouple, 6- absorber plate, 7- hot wire anemometer, 8- solarimeter).

It can be ascertained from the literature that complicated designs with internal protruding surfaces have been used that effects system hydraulic performance. The objective of the present study is to enhance the thermal performance by maintaining desired mass flow rate of air of natural convection solar air heater (SAH), without incorporating ribs and roughness on the absorber surface. The proposed curved concept designs are novel for SAH in natural convection scenario combined with chimney effect. Effect of curvature angles on thermo-hydraulic performance has been investigated.

Manufacturing of curved glass is very common in the industries like aviation, automobile, architectural designs etc. In India, cost of curved glass costs about ₹ 200/ft^{2}whereas it costs ₹ 165 ft^2 for flat glasses. The cost difference is not that significant. Clearly, the manufacturing of curved glasses are not costly vis-a-vis flat glasses. Even if it is, future generations would look for efficient designs for harnessing solar energy when non-renewable sources is completely depleted. If we consider the case of solar photovoltaics, initial costs were prohibitive for commercial applications due to higher initial cost per unit power generation. However, due to persistent effort by the scientific community and government, the technology has now become mature and commercially viable. It is expected that this chapter would provide future directions for novel research to harness solar energy efficiently.

4.2 Experimental set-up for validation

Figure 4.1 shows the experimental set-up of a conventional flat plate natural convection solar air heater reported by Gilani et al., 2017 [53]. The experimental design consists of a flat plate solar air heater, whose exit was connected to the chimney. The dimensions of flat SAH was 1100 mm in length and 950 mm in width. The distance between glass and absorber plate was 102 mm. The vertical height of the chimney was 2000 mm, which ensured that air could flow consistently over the absorber plate inside flat SAH duct. Initially, the best optimum

inclination angle of SAH was determined and it was found to be= 45° . The flat smooth passage of SAH was compared with the passage with conical pin protrusions on the absorber plate at the best optimum angle. The variation of dimensionless Nusselt number vs. Rayleigh number for different solar power input were plotted and shown the enhancement in heat transfer under natural convection, in case of flow passage with conical ribs on the absorber surface.

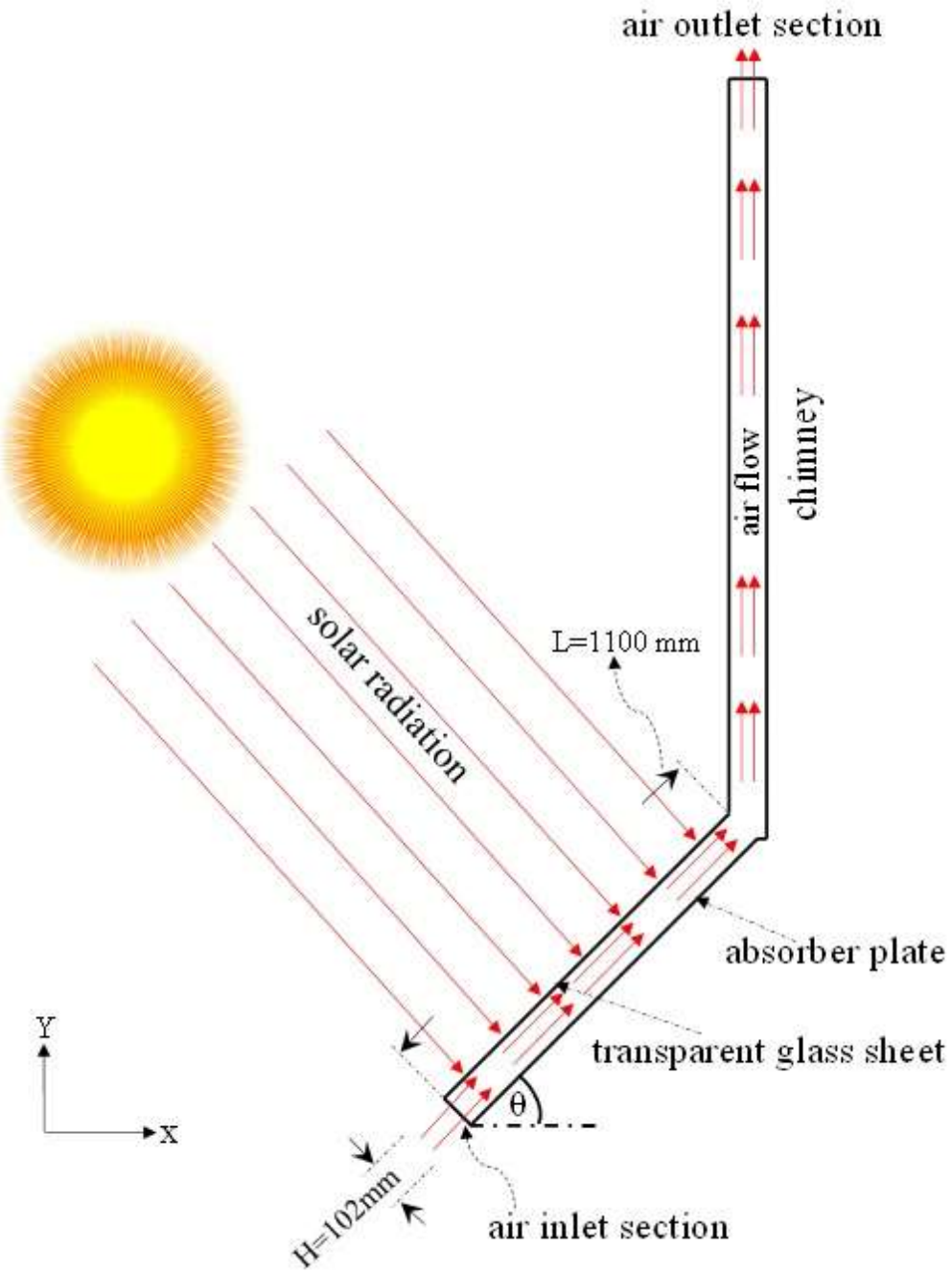

Figure 4.2: The natural convective flat SAH at an angle (θ) of 45°with respect to horizontal.

Computational fluid dynamics (CFD) model was developed having same dimensions (see Fig. 4.2) and applied the boundary conditions to mimic the experimental set-up. Design in Fig. 4.2 serves as base model for validation of the numerical model with the experimental data reported by Gilani et al., 2017 and results are compared with the new designs proposed in this chapter. All the SAH designs studied in this chapter are kept at a constant angle of = 45° w.r.t. horizontal plane throughout the study. This angle was reported to be optimum from heat transfer point of view [53]. Though there can be numerous designs of SAH without internal extended surfaces that would thermo-hydraulically perform better than conventional flat plate natural convection SAH, we report here some representative designs and their performance to encourage future innovations in designs

for efficient conversion of solar energy.

Figs 4.3 and 4.4 shows the schematic diagrams of new SAH designs, having curvature angle as design variable, that operates on natural convection principle. These concept designs are novel for SAH in natural convection scenario combined with chimney effect. The proposed designs would also serve as base design by different investigators for comparisons and further development of efficient designs. The evaluation of thermo-hydraulic performance under different sets of boundary condition for various geometrical shapes (concave and convex flow passage) were determined. A systematic procedure has been adopted, beginning with the geometrical design of the flow domain followed by proper meshing and finally developing computational models for thermo-hydraulic performance evaluation.

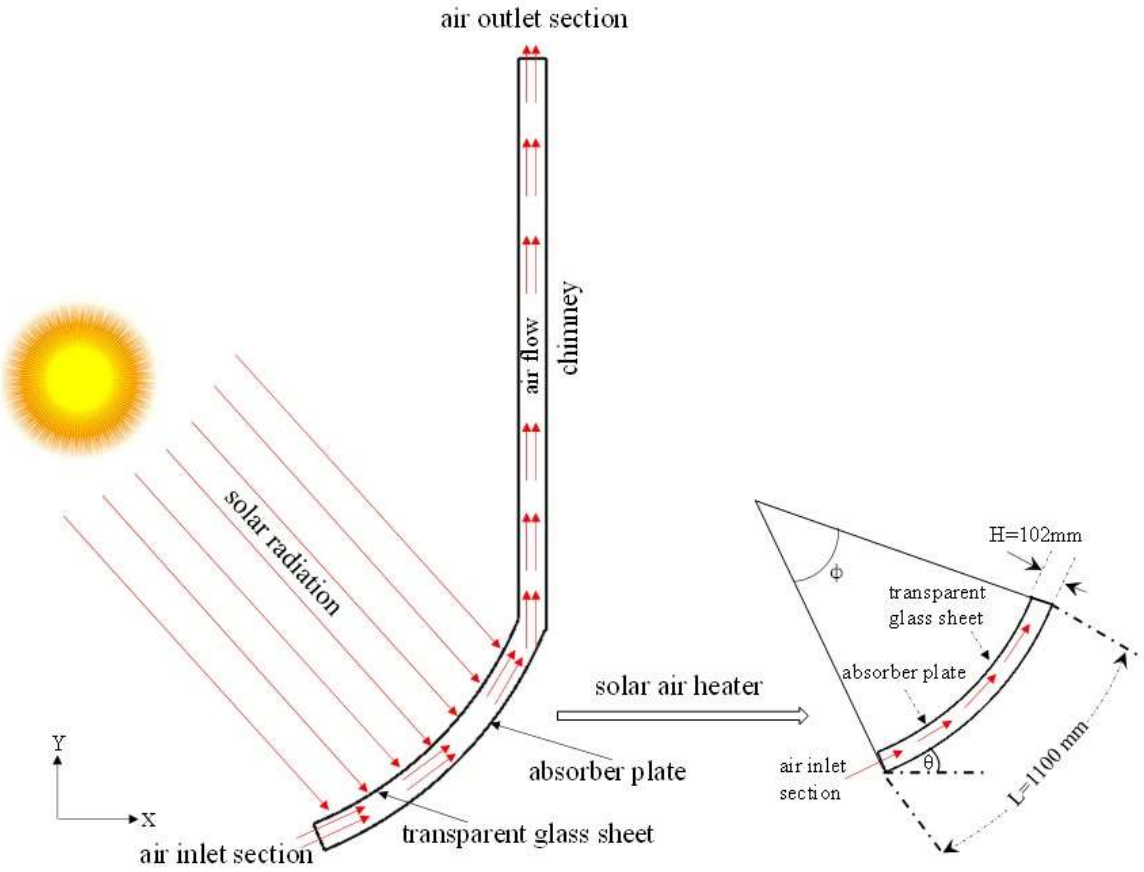

Figure 4.3: The natural convective concave curved SAH inclined at an angle (θ) of 45° with respect to horizontal plane, connected to a vertical chimney. Effect of curvature angle on thermo-hydraulic performance has been investigated.

4.3 Objective and simulation methodology

The main aim of the present study is to enhance the thermal performance of conventional flat SAH by effective design modifications. The modifications made in terms of transforming flat smooth flow channel into curved (convex and concave) channel. The gain in thermal performance has been achieved without creation of roughness (ribs/turbulators) in the flow channel. Both the convex and concave flow channels have been analyzed separately in the result section. The steps involved the numerical analysis pre-processing and post-processing. The pre-processing involved designing the geometry, mesh generation and applying suitable boundary conditions. Results were post-processed after convergence is achieved.

4.3.1 New SAH designs

4.3.2 Selection of physics models and governing equations

The computational flow domain is discretized into optimum number of small size elements in order to study the air flow movement and heat transfer characteristics using finite volume method. After implementing boundary conditions, the thermal performance in terms of outlet air temperature (T_o) and Nusselt number (Nu) have been obtained numerically for different cases. The Nusselt number and heat transfer coefficient values have been calculated numerically at surface of the absorber plate. The dependent variable was the dimensionless Nusselt number obtained using Eq. 4.1 [68, 119].

$$Nu = \frac{h_{avg}\ L_c}{k_a} \tag{4.1}$$

where h_{avg} is the average convection heat transfer coefficient $= \frac{1}{A}\int_A \frac{q_{Conv}}{(T_s - T_a)} dA$

L_c is the height of the air flow duct passage (i.e. distance between the top glass and absorber plate), h is the convective heat transfer coefficient from hot absorber surface to fluid medium (air) and k_{a} is the thermal conductivity of air.

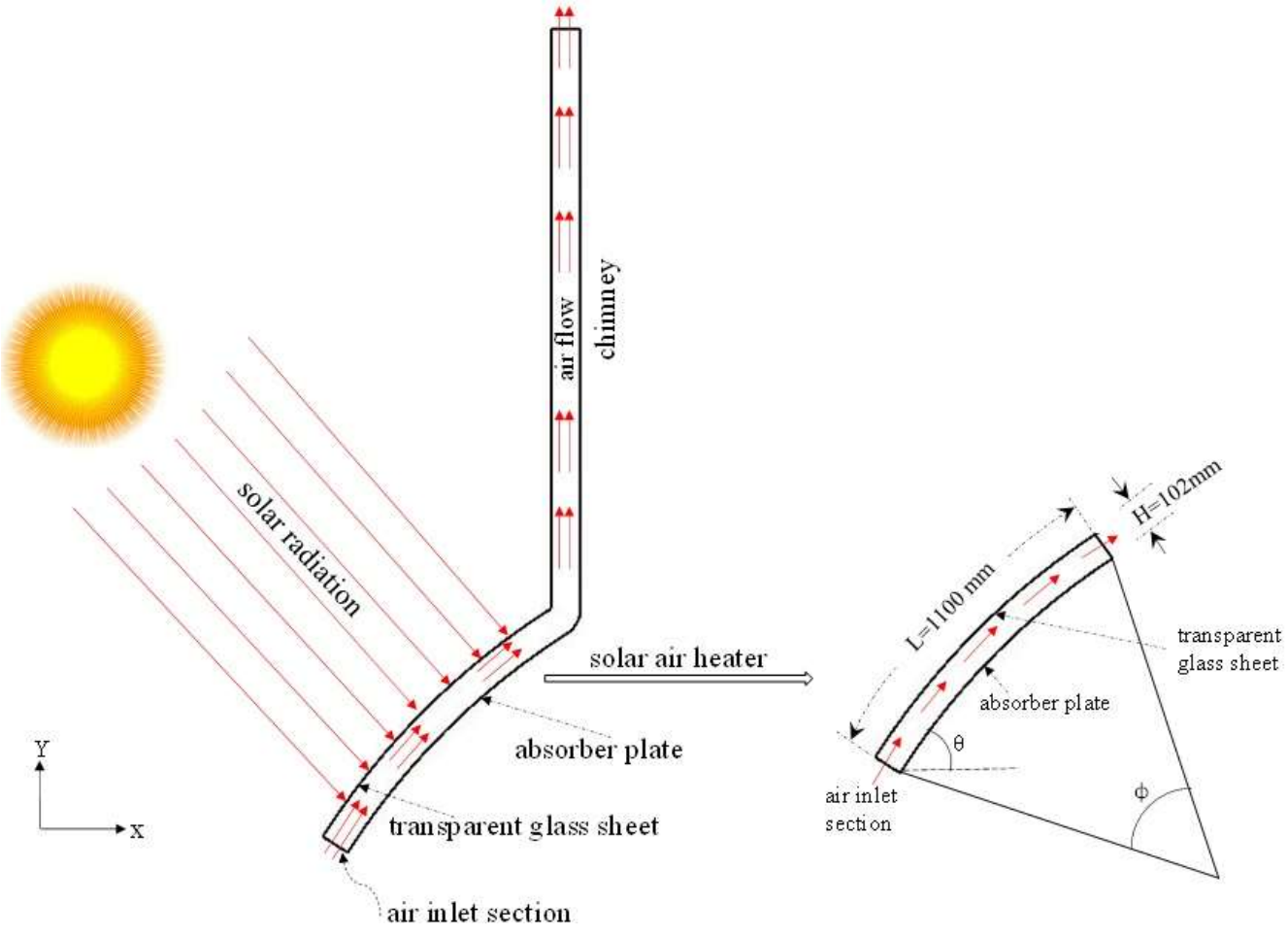

Figure 4.4: The natural convective convex curved SAH inclined at an angle (θ) of 45°with respect to horizontal plane, connected to a vertical chimney. Effect of curvature angle on thermo-hydraulic performance has been investigated.

In the natural convection SAH, the change in buoyancy drives the flow movement, and hence the dimensionless Rayleigh number (Ra) has been considered instead of Reynolds number (Re). The Rayleigh number was calculated using basic Eq. 4.2 [68, 119, 63].

$$Ra = \frac{\rho^2 \beta C_P g \Delta T L^3}{\mu k_a} \tag{4.2}$$

where ρ is the density of air, β is the volumetric expansion coefficient (K^{-1}), μ is the dynamic viscosity

of air (Ns/m^2), $\Delta T = T_s$–T_a (K) where T_s = mean surface temperature of absorber plate surface (K) and T_a= air temperature at the inlet section (K), g is the gravitational constant (m.s^{-2}), C_P is the specific heat of air (J/kg.K), L is the length of the absorber plate and k_a is the thermal conductivity of air (W/m.K). Heat transfer model was used instead of radiation model to capture flow behaviour inside the SAH [124]. To account for the radiation losses, equivalent radiation heat transfer coefficient was imposed on the top glass surface. The dimensionless Rayleigh number has a governing term which is directly proportional to the temperature of absorber surface, higher the temperature of absorber surface more air would pass through SAH duct. It helps to distinguish between laminar and turbulent flow in cases when the flow occurs due to natural convection.

In the present study, the values of Rayleigh number was found to be of the order more than 10^9 ($Ra > 10^9$) which comes under turbulent flow range, and hence the Realizable K-Epsilon model with the two-layer approach has been used in the simulations [110, 124]. The Realizable K-Epsilon model gains the added flexibility of an all dimensionless wall distance y^+ wall treatment. A very fine boundary layer mesh region generated near walls with the intention of resolving the laminar sub-layer, near walls the dimensionless wall distance has been found less than unity. The flow domain is discretized using finite volume method (FVM) in order to study two-dimensional, ideal gas, unsteady state flow movement of air and its heat transfer characteristics. The results were recorded when the values of parameters attains steady value and insensitive of successive time steps. The following sets of governing equation i.e. continuity, X- and Y- momentum and energy equations [124, 116] were solved for two-dimensional computational domain.

Continuity equation,

$$\frac{\partial \rho}{\partial t} + \frac{\partial (\rho u)}{\partial x} + \frac{\partial (\rho v)}{\partial y} = 0 \tag{4.3}$$

Momentum equations,

$$\frac{\partial (\rho u)}{\partial t} + \frac{\partial (\rho u u)}{\partial x} + \frac{\partial (\rho u v)}{\partial y} = -\frac{\partial p}{\partial x} + \frac{\partial}{\partial x}\left[(\mu + \mu_t)\frac{\partial u}{\partial x}\right] + \frac{\partial}{\partial y}\left[(\mu + \mu_t)\frac{\partial u}{\partial y}\right] - \frac{2}{3}\rho\frac{\partial k}{\partial x} \tag{4.4}$$

$$\frac{\partial (\rho v)}{\partial t} + \frac{\partial (\rho u v)}{\partial x} + \frac{\partial (\rho v v)}{\partial y} = -\frac{\partial p}{\partial y} + \frac{\partial}{\partial x}\left[(\mu + \mu_t)\frac{\partial v}{\partial x}\right] + \frac{\partial}{\partial y}\left[(\mu + \mu_t)\frac{\partial v}{\partial y}\right] - \frac{2}{3}\rho\frac{\partial k}{\partial y} - (\rho - \rho_0)\, g \tag{4.5}$$

Energy equation,

$$\frac{\partial (\rho T)}{\partial t} + \frac{\partial (\rho u T)}{\partial x} + \frac{\partial (\rho v T)}{\partial y} = \frac{\partial}{\partial x}\left[\left(\frac{K}{C_P} + \frac{\mu_t}{\mathrm{Pr}_t}\right)\frac{\partial T}{\partial x}\right] + \frac{\partial}{\partial y}\left[\left(\frac{K}{C_P} + \frac{\mu_t}{\mathrm{Pr}_t}\right)\frac{\partial T}{\partial y}\right] \tag{4.6}$$

Where k is the turbulent kinetic energy, μ_t is the turbulent viscosity and Pr_t is the turbulent Prandtl number which is the ratio of eddy diffusivity for momentum $\left(\varepsilon_M = \frac{\overline{-u'v'}}{\frac{\partial \overline{u}}{\partial y}}\right)$ and heat transfer $\left(\varepsilon_H = \frac{\overline{-v'T'}}{\frac{\partial \overline{T}}{\partial y}}\right)$.

The SIMPLE (semi-implicit method for pressure linked equations) algorithm is used to solve velocity and pressure fields for the discretized computational flow domain. The criteria for convergence was set to the order 10^{-3} for energy equation and 10^{-5} order for velocity component and momentum equations.

4.3.3 Basic design details of geometry and parameters

The study of two-dimensional model considered for the computational domain of a natural convective SAH having rectangular cross-section throughout along the air flow passage which connects inlet and outlet, respectively. The dimensions of flat natural convective SAH having length and height of 1100 mm and 102 mm, respectively and the height of the vertical chimney attached at the exit of SAH is 2000 mm long with an opening thickness at the outlet is 102 mm to ensure proper consistent air flow movement as shown in Fig. 4.2. The same geometrical design of flat SAH was reported in the literature [53]. In the present study, all the surfaces of curved SAH are kept same as that of flat SAH. Curved SAH are designed from flat SAH by providing suitable curvature in the design software.

The numerical model comprises of air inlet, top glass glazing, bottom absorber surface, chimney at the exit of SAH and air outlet. The absorber plate has been exposed to constant heat flux (q) condition. At the inlet

of SAH, air automatically gets sucked in the flow channel due to buoyancy forces and gradually absorbs heat from the hot absorber surface, which is exposed to constant heat flux. The heated air rises upward due to density difference in the SAH duct. The chimney attached at the exit of SAH guides the air flow movement. The basic geometrical parameters i.e. range of curvature angle of concave and convex curved flow passage, respectively have been listed in the Table 4.1. Simulations have been performed for different values of absorber heat flux. The numerical results obtained for different cases were compared with the conventional flat plate natural convective SAH.

Table 4.1: Curvature angle and boundary conditions.

S. No.	Parameters	Values of parameters
1	Curvature angle (ϕ) of curved air flow passage	25° , 30° , 35° , 40° , 45° , 50°
2	Absorber heat flux (q) in W/m^2	500, 600, 700, 800, 900, 1000, 1100
3	Inlet condition	$P_{total} = 0$ (stagnation pressure condition)
4	SAH inclination angle w.r.t. horizontal plane (θ)	45°(fixed)
5	Convection heat transfer coefficient of top glass plate was determined by $h = 5.7 + 3.8V_\infty$ (W/m^{2}K)	5.7 (Sukhatme, 2008)

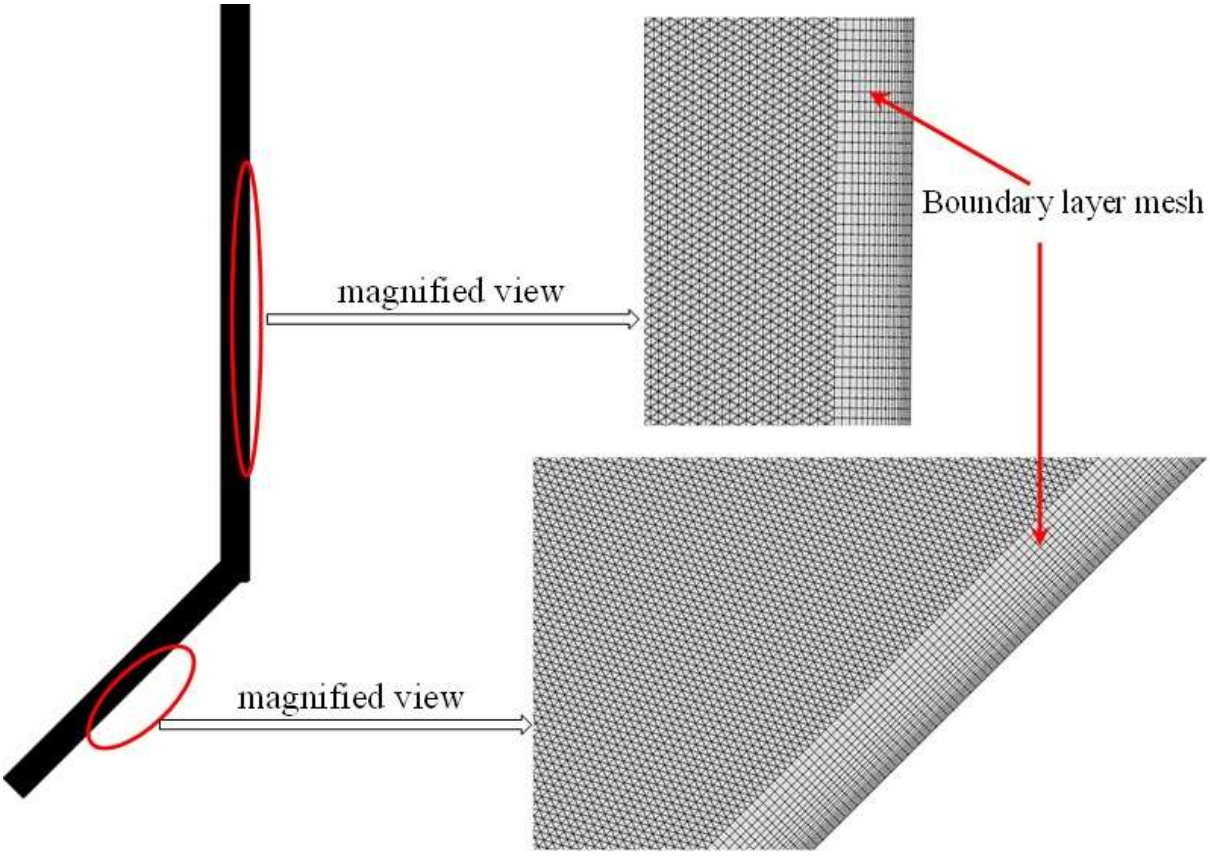

Figure 4.5: Computational mesh domain of the flat natural convective SAH. Boundary layer mesh is shown in the magnified views.

4.3.4 Methodology of mesh generation and grid independent test

The method adopted to mesh the computational domain as such to have an optimum accuracy of results obtained in minimum possible computational time and resources. Two-dimensional unstructured mesh were generated to discretize the computational flow domain. For more complex geometries an unstructured mesh possess better tendency to capture secondary flow vortices compared to conventional mesh (Singh and Singh, 2018; Pirzadeh, 2001). Fine structured mesh with multiple boundary layers adjacent to walls was created along the flow passage to visualize the air flow patterns due to buoyancy effect as shown in Fig. 4.5. This helps in accurately predicting the pressure losses in boundary layer and flow vortices formation near to the wall of absorber plate. The dimensionless wall distance (y^+) has been found less than unity. The model of flat SAH has been tested for trias and quad shape mesh elements in core flow region. The results were showing insignificant change in the parametric values for the same number of elements.

Table 4.2: Details of grid independent test.

Mesh type	Element shape	S. No.	Number of elements	Percentage variation in Nusselt number (Nu)
Unstructured	Trias	1	81000	–
		2	118123	1.79
		3	154873	0
		4	274954	0.27

In the grid independent test, appropriate grid sizes were chosen to achieve accurate results in minimum processing time. The grid independent test has been conducted for different number of elements in the range of 81000 to 274954, respectively for flat plate convective SAH inclined at 45° w.r.t. horizontal plane. The exit of the SAH is attached to chimney of 2000 mm in length to guide the flow upward to ensure consistent air flow in the flow passage of SAH under natural convection. The outcomes obtained numerically were recorded in terms of percentage variation of Nusselt number (Nu) are shown in Table 4.2. The percentage variation in the Nu are 1.79% , 0% and 0.27% when the number of elements increases from 81000 to 118123, 118123 to 154873 and 154873 to 274954, respectively. The variation in the results are insignificant, and hence the number of optimum elements has been considered as 118123 for all mentioned cases. Refer appendix A for more procedural details related to grid and time independent test.

4.3.5 Boundary conditions and experimental validation

The flow passage of convective SAH comprised of air inlet section, top glass glazing, bottom absorber surface, chimney at the exit of SAH and finally air exit through the outlet section situated at top end of the chimney. The air inlet section was assigned to stagnation pressure condition which is equivalent to environmental condition, the air enters the inlet section due to buoyancy effect created by hot bottom absorber surface. Such boundary condition is preferred for buoyancy driven flows where neither the flow rate nor the velocity are known at the inlet section. The bottom absorber plate was set to a constant heat source. The chimney outlet section was kept as outlet condition which represents an outflow condition where no backflow occurs. The top glass plate (glazing) was set to convection heat transfer which represents convection heat loss in respect of environment condition, in order to ensure the conditions more practical to match experimental condition. The heat transfer coefficient value was assigned to top glass surface of SAH to allow heat loss from top glass surface to surroundings [150]. Atmospheric wind velocity V was taken as zero and hence $h = 5.7$ W/m^{2}K (see Table 4.1). In natural convection where ambient wind speed is negligible, equivalent radiation heat transfer coefficient is same as convection heat transfer coefficient [150]. Rest of the walls and the chimney surfaces were considered as adiabatic and assigned to no-slip boundary condition.

In our study the temperature difference of the walls is more than 30° C. For the case, when the temperature difference is up to 30° C, Boussinesq approximation can estimate the heat transfer with about 1% error. However, for the temperature difference more than 30° C, a significant deviation in flow configuration is observed in the Boussinesq solution, affecting the thermal stratification and heat transfer. Under such conditions Boussinesq approximation may lead to incorrect predictions of the phenomenon taking place [85, 168]. A gas generally

behaves more like an ideal gas at low pressure and high temperature, as the potential energy due to the intermolecular forces in between particles are less significant when compared with particles kinetic energy, as the molecules size is less considerable compared to space between them. Hence, the air has been considered as an ideal gas for the present study.

Air possess low thermophysical properties, so for small rise in atmospheric temperature, all physical properties are assumed to be constant at 298 K temperature (environmental condition) at the inlet section are listed in Table 4.3.

Table 4.3: Thermo-physical properties of air at 298 K at the inlet of SAH.

Properties name	Value
Dynamic viscosity (μ)	1.855 x 10-5 Ns/m^2
Thermal conductivity (k)	0.026 W/m K
Prandtl number (Pr)	0.71
Specific heat (C_p)	1003.62 J/kg K
Density (ρ)	1.184 kg/m^3

The results obtained numerically were validated with the experimental results of the literature Gilani et al., 2017 [53]. They reported maximum error in calculating Nusselt number as 9.1% and mean percentage of error in the entire data range of Nusselt number were 6.4% . The values of Nusselt number corresponding to hydraulic diameter $0.122m$ were obtained for different values of Rayleigh number, Ra as shown in Fig. 4.6. The Ra values shown in validation results were obtained corresponding to characteristic length 0.102 m i.e. the height of the SAH duct and $\Delta T = (T_o - T_a)$, i.e. same as reported in the literature [53]. The percentage variation of Nusselt number has been found to be in the range of $0.08 - 9.4\%$. Since these variations are within the accepted limits, the numerical model can be considered to be validated. Further design studies have been explored with the same validated model. Note that the values of Nusselt number in the result sections below are reported using the height of the SAH duct i.e. $0.102\,m$, and Rayleigh number values are reported corresponding to characteristic length i.e. absorber plate length $1.1\,m$ and temperature gradient $\Delta T = (T_s - T_a)$ [91].

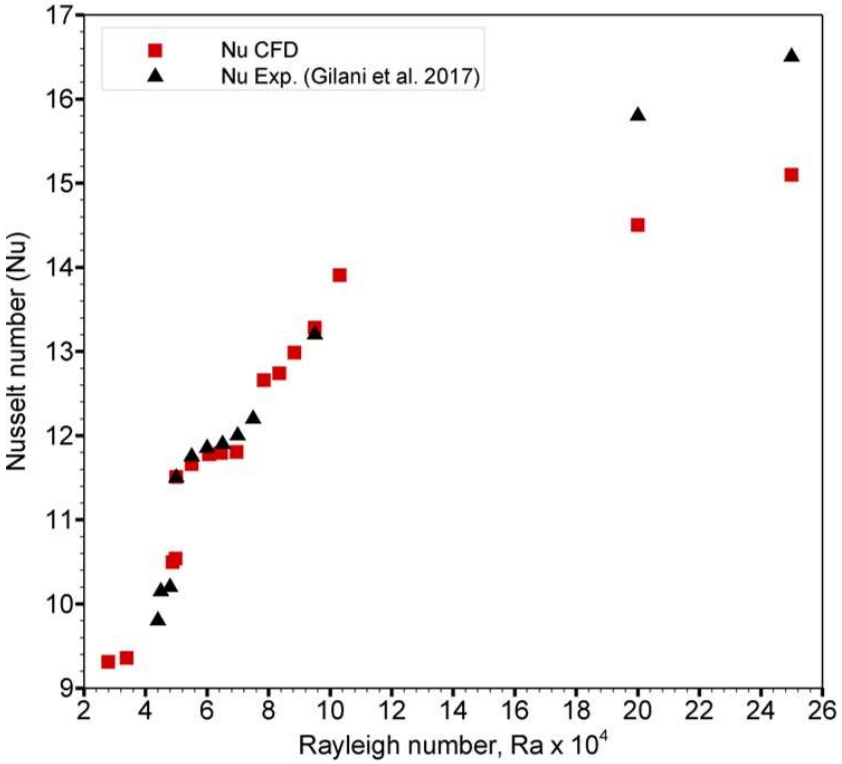

Figure 4.6: Validation of computation flow model with the experimental data of the literature (Gilani et al., 2017).

4.4 Results and discussions

The results are presented in terms of variations in Nusselt number (Nu), outlet air temperature (T_o), effectiveness (ε) and mass flow rate (m) for different geometric configurations considered in the present analysis. The variation of temperature enhancement ratio (TER) and heat transfer enhancement factor ($HTEF$) were shown to manifest the enhancement in thermal performance associated with modified geometries over conventional flat natural convective SAH. HTEF and TER are defined as:

$$HTEF = \frac{Nu_{curved}}{Nu_{flat}} \tag{4.7}$$

$$TER = \frac{T_{curved}}{T_{flat}} \tag{4.8}$$

The boundary conditions were kept same in the analysis throughout. The increasing values of Nusselt number represents the higher heat transfer rate from hot absorber surface to air passing through the SAH duct. The increasing value of heat carrying capacity of air consequently increases the outlet air temperature (the desired output for heating applications). The variation of thermal parameters have been recorded with respect to various values of absorber heat flux in the range of 500-1100 W/m^2. The outcomes of curved geometries i.e. concave and convex natural convective SAH are discussed below in detail.

4.4.1 Effect of concave and convex curved designs on thermal performance

The geometry of flat straight passage of SAH duct has been modified to concave and convex curved passage of natural convective solar air heater. We studied the effect of six different curvature angle (ϕ) in the range of 25°–50° , for both concave and convex geometries separately are shown in Figs. 4.3 and 4.4, respectively. The effect of curvature angle have been recorded and seen considerable enhancement in the thermal performance when compared with the conventional flat plate natural convective SAH, in terms of outlet air temperature, dimensionless Nusselt number and effectiveness. The Figs. 4.7, 4.8 and 4.9 shows variation of temperature enhancement ratio (*TER, i.e.* $T_{o,\text{ curved}}$ / $T_{o,\text{ flat}}$), heat transfer enhancement factor ($HTEF$) and mass flow rate w.r.t. absorber heat flux. When the buoyant air moves upward in the convex design of SAH, it deflects the air downwards i.e. against the gravity which intensifies the mixing of the flow and hence, more heat transfer occurs. However, in case of concave design, the flow is diverted upwards resulting in less mixing between hot and cold layer of fluids. The warm air having tendency to move upwards and because of centrifugal effect, the rising air interact more frequently due to formation of secondary flow vortices (refer Fig. 4.12 and 4.13) with the hot absorber surface, and hence heat transfer rate enhances. The Figs. 4.7 and 4.8 demonstrates, how much effective are the concave and convex- curvature designs for natural convection SAH over conventional flat plate designs. The thermal performance of curved flow passage is significantly higher for the values of curvature angle i.e. 25°, 30°, 35°, 40°, 45° and 50°, for both concave and convex flow passage. For the case of convex curvature flow channel having 30° curvature angle possess maximum enhancement in thermal performance, while it is 40° for the concave curvature flow channel.

It was observed that the flow of air begins from the air inlet section, when the ambient air comes in contact with hot absorber surface. The movement of heated air has tendency to move upwards due to buoyancy force in the flow passage of duct of solar air heater. The latter half portion of curved flow passage is in continuous contact with the curved hot absorber surface. As centrifugal forces induce the formation of secondary vortices, mixing of air in the flow enhances thermal performance of curved natural convection SAH. In case of convex design, the flow of air has tendency to shifts towards outer periphery (i.e. glass glazing), heated air naturally moves upwards and layers of fresh envelope of air (i.e. unheated air) gets entrained near the hot absorber surface. Consequently, the average temperature of heated air at the outlet section increases. While in case of concave designs, the buoyant air has the tendency to move towards hot absorber surface due to centrifugal action, and hence the fresh air at the top glass side do not frequently interact with the absorber. So, the convex curved flow passage is slightly thermally more effective compared to concave curved flow passage under same sets of boundary conditions.

Figure 4.9 shows the variation of Nu w.r.t. temperature factor, $\frac{(T_o - T_i)}{I}$, for flat and different curvature angle

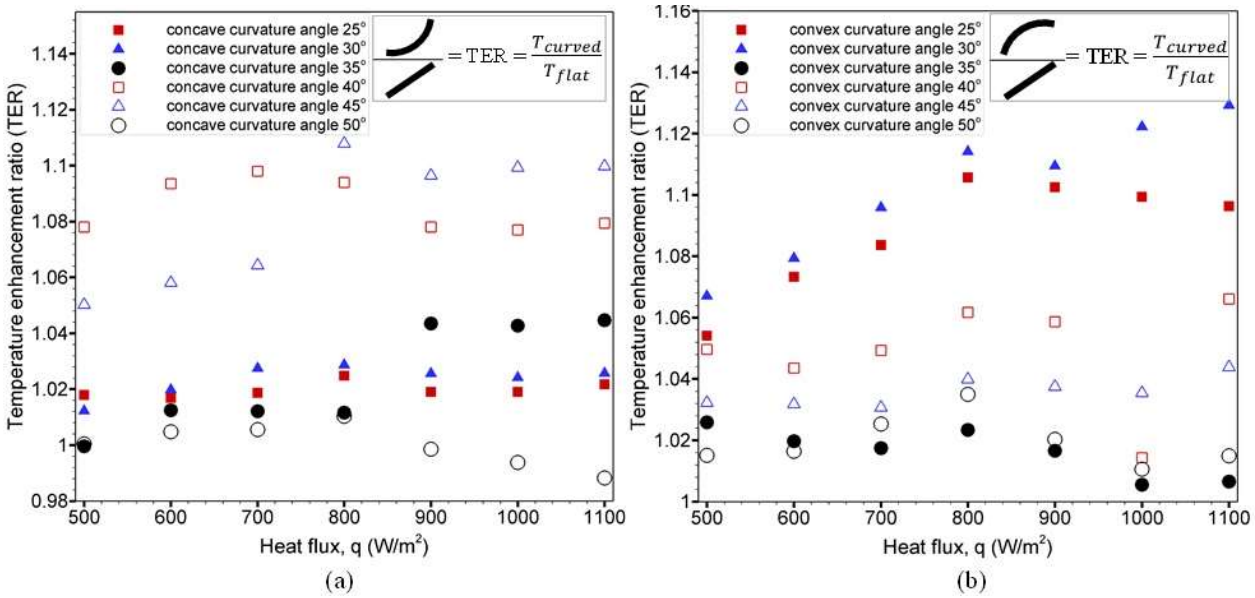

Figure 4.7: Variation of TER of: (a) concave curved natural convective SAH; (b) convex curved natural convective SAH, for six different curvature angle in the range of 25°-50°.

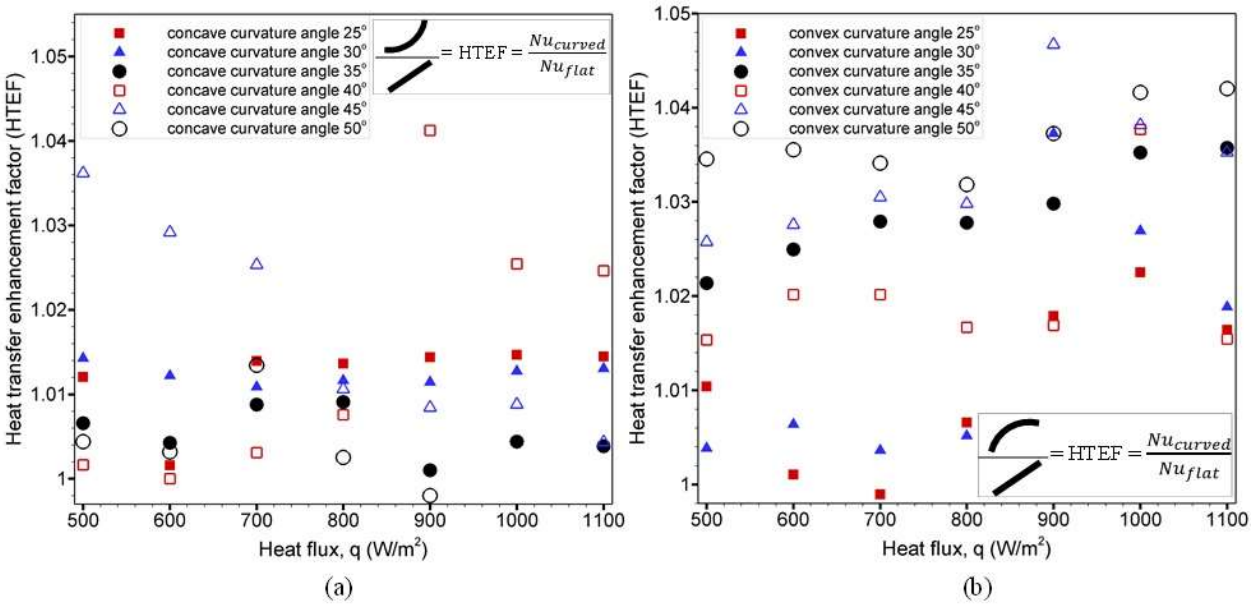

Figure 4.8: variation of HTEF of: (a) concave curved natural convective SAH; (b) convex curved natural convective SAH, for six different curvature angle in the range of 25°-50°.

(30°, 40° and 50°) of concave and convex natural convective SAH, at different values of constant absorber heat flux in the range of $500 - 1100$ W/m^2. Both curved (concave and convex) SAH shows substantial improvement in the heat transfer characteristics, compared to conventional flat SAH. The values of temperature factor and Nusselt number for the convex SAH were found to be significantly higher than the conventional flat and concave SAH design. The enhancement of thermal characteristics is due to the convex curvature effect, which initially assist the upward flow movement of hot air at the first half in the SAH duct, and thereby enhance the Nusselt number for convex flow channel. Each curvature angle possess different heat transfer characteristics, due to diverse curvature effect. The curvature of curved SAH greatly influence the buoyancy (gravity) driven flow, and hence the thermal performance. The results for both concave and convex SAH are encouraging in terms of thermal performance in comparison to conventional flat SAH.

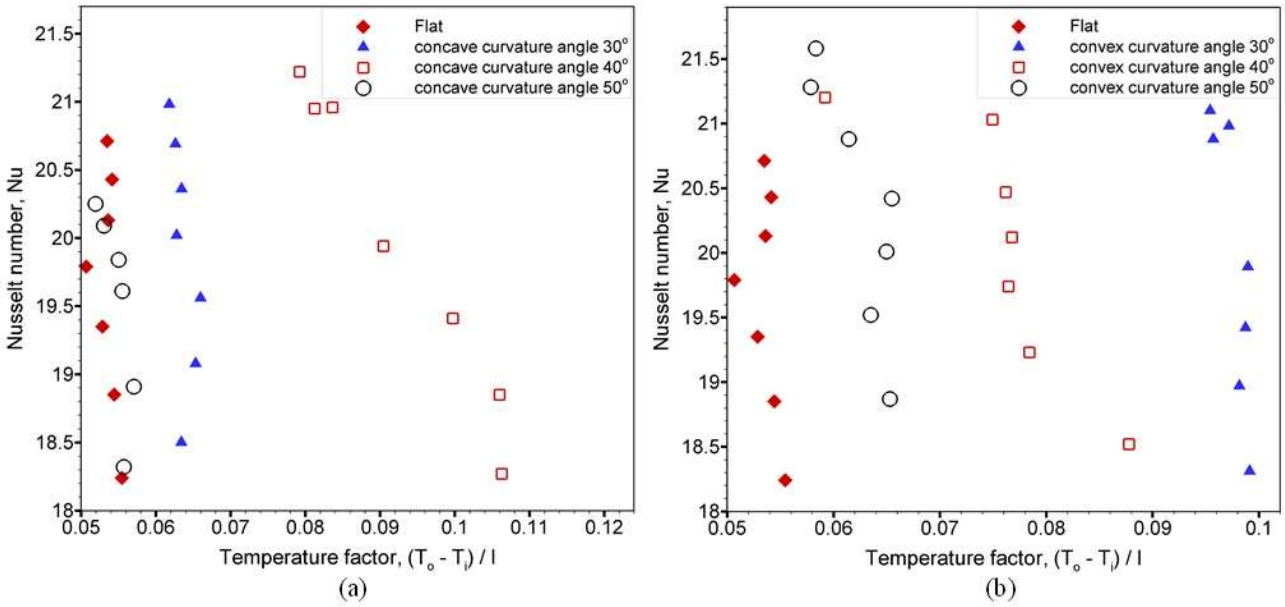

Figure 4.9: Variation of Nu w.r.t. temperature factor, $\frac{(T_o - T_i)}{I}$, of flat and different curvature angle (30°, 40° and 50°) of: (a) concave curved natural convective SAH; (b) convex curved natural convective SAH, at different values of constant absorber heat flux in the range 500-1100 W/m^2.

The thermal performance of a solar air heater can be defined in terms of effectiveness, which is the ratio of actual temperature gain to maximum possible temperature gain [68], i.e.

$$\varepsilon = \frac{(T_o - T_i)}{(T_s - T_i)} \tag{4.9}$$

Table 4.4: Average effectiveness values for convex, concave and flat natural convective SAH at constant absorber heat flux for range 500-1100 W/m^2.

Curvature angle (ϕ) →	25°	30°	35°	40°	45°	50°
SAH ↓						
Convex curved	0.449	0.464	0.309	0.372	0.348	0.313
Concave curved	0.312	0.318	0.310	0.442	0.425	0.267
			average effectiveness (ε) ↓			
Flat (conventional)			0.263			

Figure 4.10 shows the effectiveness of concave and convex flow designs of natural convection SAH. The convex curved natural convective SAH shows maximum average effectiveness of 0.464 at 30° curvature angle while it is 0.442 for concave curved at 40° curvature angle, which is 76.42% for convex and 68.06% for concave, higher than the conventional flat SAH design. Table 4.4 lists average effectiveness data of three different (concave, convex, and flat) natural convective SAH models considered in the present study. On average, both convex and concave-curved geometries are 42.91% and 31.43% , respectively, thermally more effective compared to conventional flat natural convective SAH. The SAH with convex curved flow passage is highly effective compared to concave

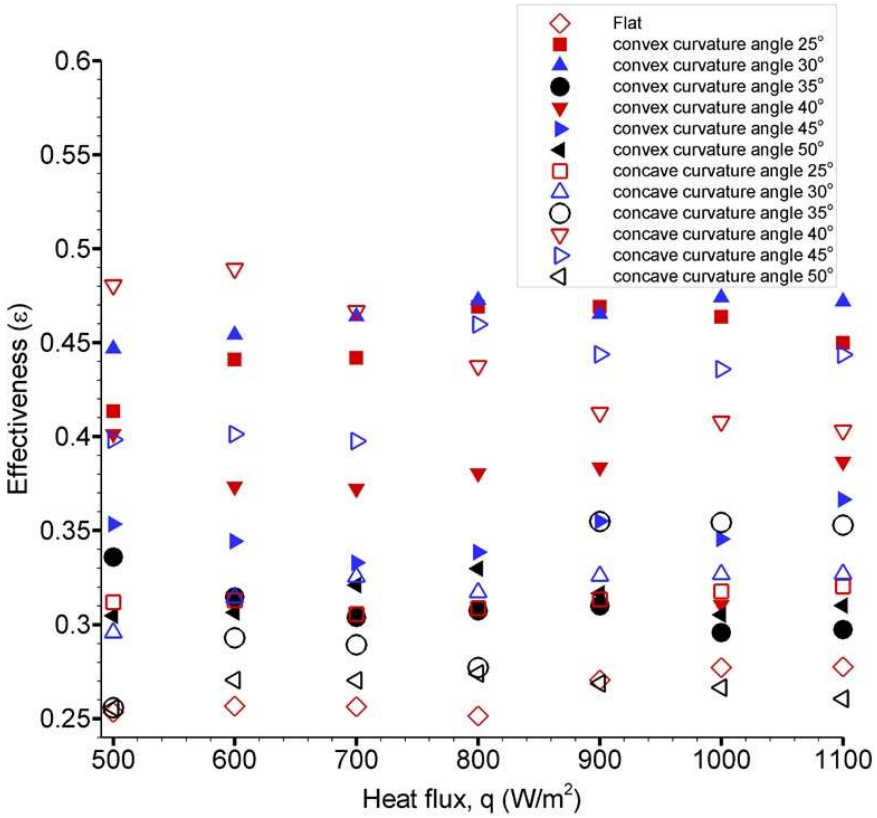

Figure 4.10: The plot shows effectiveness of concave and convex curved and flat- flow passage of natural convective SAH with respect to different values of constant absorber heat flux.

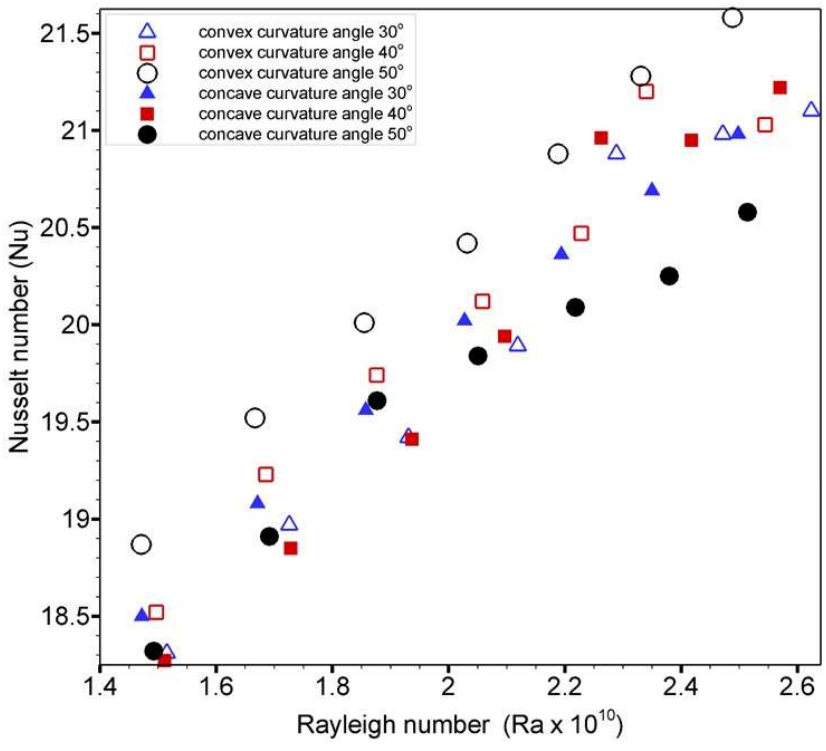

Figure 4.11: Shows the variation of Nu vs. Ra of concave and convex curved- SAH at all value of heat flux in the range of 500-800 W/m^2.

due to formation of secondary flow vortices because of centrifugal action. Consequently, mixing in the air flow increases and resulting higher temperature at the chimney outlet.

Figure 4.11 shows the variation of Nusselt number w.r.t. Rayleigh number. The convex curved SAH possess maximum value of Nu at specific value of Ra. The variation trend of convex curved SAH are analogous to each other with negligible difference for various curvature angles in the range of 25°-50°. The next higher values of Nu have been seen for concave SAH. Clearly, the alternative designs of SAH discussed in this chapter have been found to have high thermal performance in comparison to conventional flat SAH working on natural convection.

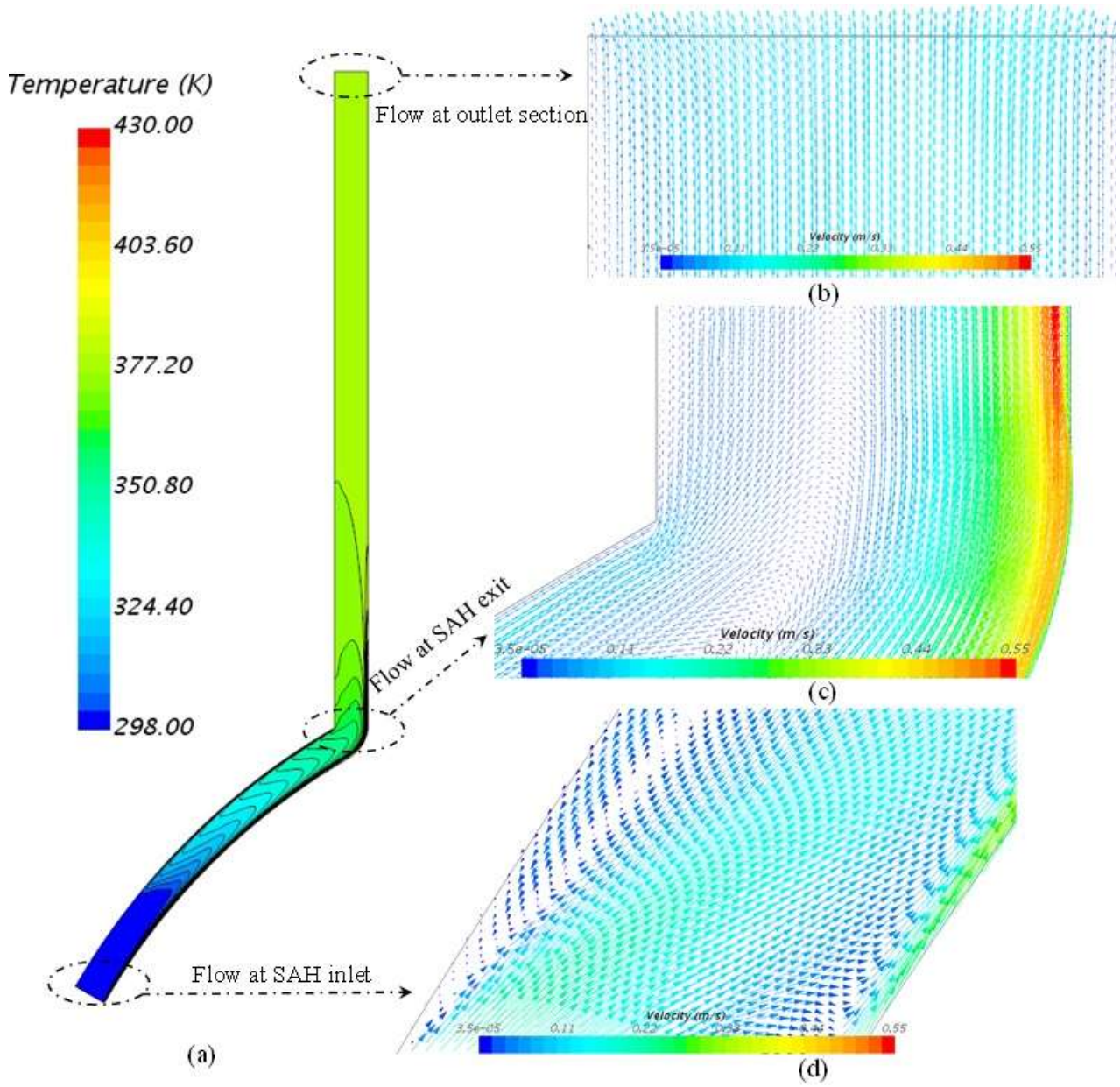

Figure 4.12: The temperature and velocity contours have been shown for convex SAH having best curvature angle 30° at constant absorber heat flux of 800 W/m^2. (a) Temperature contours; Velocity contours at (b) chimney outlet, (c) SAH exit and (d) SAH inlet section. Similar contours were observed for other curvature angles.

The pressure drop (ΔP) and the Nusselt number per unit pressure drop, NuP (Nu/ΔP) values of various SAH designs at constant absorber heat flux of 800 W/m^2 have been shown in Table 4.5. The average percentage decrease in pressure drop for convex and concave designs are 4.45% and 4.67%, in comparison to the conventional flat SAH design. The corresponding increase in average effectiveness are 42.91% and 31.43%, respectively, in comparison to conventional flat SAH. The pressure drop across the flow channel of smooth flow passage is comparatively much lower than the SAH equipped with various shape of ribs [68, 119, 145, 125, 90, 108]. The ratio NuP represents the heat carrying capacity of air flow from the hot absorber plate at the expense of pressure

drop. Higher the ratio value, higher would be the mass flow rate and outlet air temperature. The values of NuP are maximum for convex curved SAH with a maximum percentage increase of 9.43% w.r.t. conventional flat plate SAH, while it is 9.88% for concave curved SAH. The convex SAH possess maximum effectiveness in terms of heat gain by the air with minimum frictional losses.

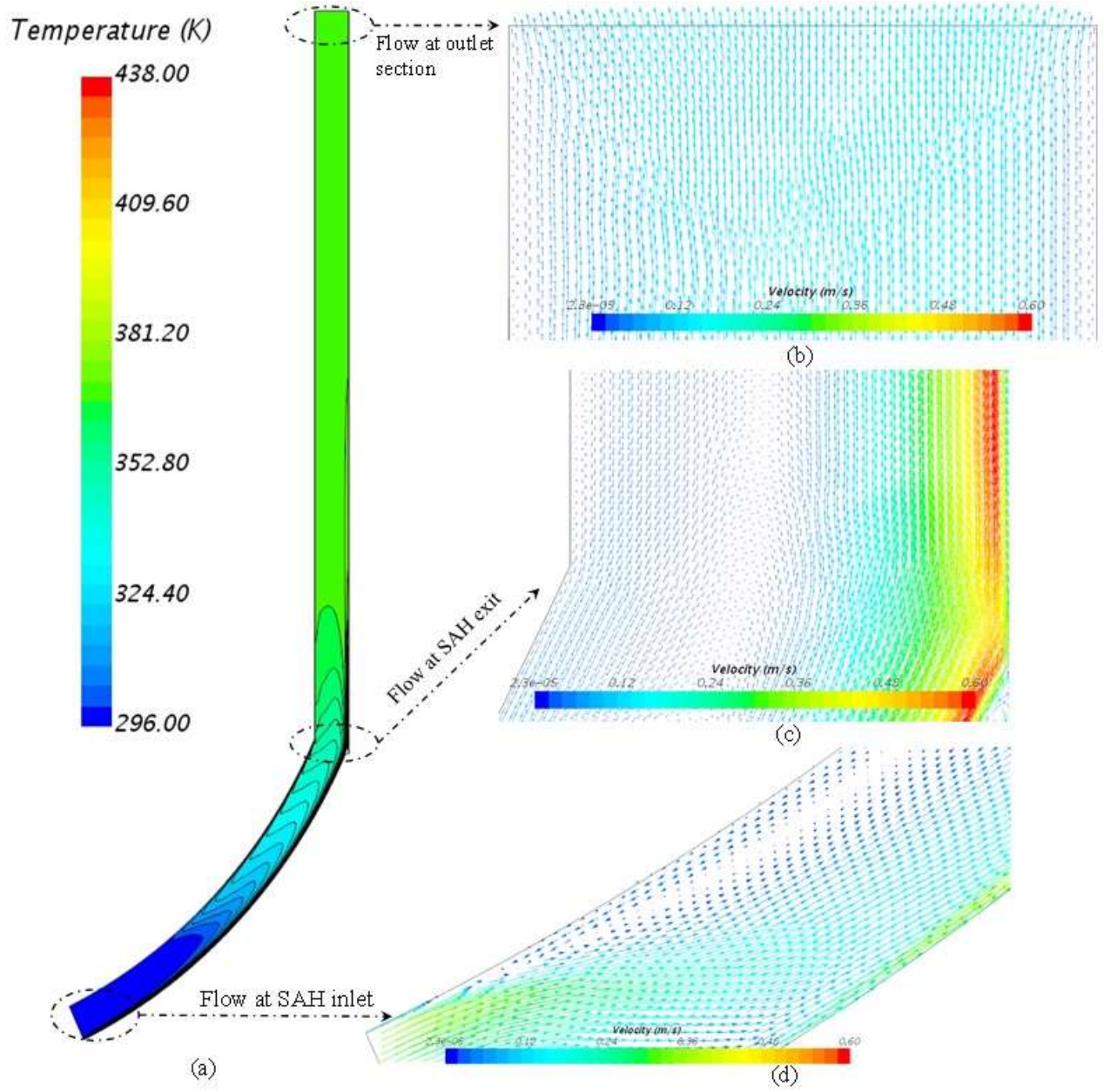

Figure 4.13: The temperature and velocity contours have been shown for concave SAH having best curvature angle 40° at constant absorber heat flux of 800 W/m^2. (a) Temperature contours; Velocity contours at (b) chimney outlet, (c) SAH exit and (d) SAH inlet section. Similar contours were observed for other curvature angles.

The Figs. 4.12 and 4.13 shows temperature and velocity contours of convex (30°) and concave (40°) natural convection SAH, respectively, when the absorber has been set to a fixed constant heat flux of 800 W/m^2. The velocity of air increases as the flow proceeds along the flow passage. Due to high temperature and velocity gradient near the absorber surface, adjacent fluid layers gets heated up and drags up quiescent fluids thereby increase the velocity. It can be seen that even if air recirculates and separates at the SAH exit (Fig. 4.12 c), it becomes uniform by the time it reaches chimney exit (Fig 4.12 b). One interesting observation is observed at the inlet section of SAH (see Fig. 4.12 d). Cold ambient air tends to rush towards the heated plate thereby forcing fluid from the top to move back, resulting in circulation loop formation. This in turn increases the interaction with the heated fluid and hence results in high exit temperature. By the time fluid teaches the chimney exit section the temperature and fluid velocity becomes uniform. Similar behaviour was observed for concave design

of SAH (Fig. 4.13).

Table 4.5: (ΔP) and (NuP) values for convex and concave curved- natural convection SAH at constant absorber heat flux of 800 W/m^2.

Curvature angle (ϕ) →	25°	30°	35°	40°	45°	50°
SAH ↓			(ΔP) in Pa ↓			
Convex curved	27.8	27.18	29.10	28.23	28.68	28.76
Concave curved	28.84	28.69	29.03	27.15	26.8	28.84
			(NuP) ↓			
Convex curved	0.716	0.731	0.698	0.712	0.710	0.710
Concave curved	0.695	0.697	0.687	0.734	0.746	0.687
			(ΔP) in Pa ↓			
Flat (conventional)			29.61			
			(NuP) ↓			
Flat (conventional)			0.668			

4.5 Correlation development

In the previous sections, it has been observed that the thermal performance is a strong function of Rayleigh numbers, Ra and curvature angle, for different designs of SAH while operating on natural convection principle. Since both the designs of SAH for wide range of design variables have been investigated and hence, two individual correlations have been developed for each. i.e. concave and convex SAH. It is to be noted that for better correlations development, minimum 10 data points are considered appropriate per variables. In this chapter, we have used 22 data points for each variable. The functional relationship of Nusselt number with the influencing parameters may be of the following form:

$$Nu = F[(Ra\,cos\theta),\ \phi] \tag{4.10}$$

4.5.1 Correlation development for concave designs of SAH

The influencing parameters for the concave designs of SAH were Rayleigh numbers and curvature angle. The functional form of Nusselt number variation can be expressed as 4.10,

To obtain the relationship among Nusselt number (Nu) and Rayleigh number (Ra), the plot of logarithmic ln(Nu) verses ln(Ra cosϑ) were plotted for different values of Rayleigh number (Ra) at respective absorber heat flux (q) in the range of 500–1100 W/m^2 as shown in Fig. 4.14. The relationship between ln(Nu) verses ln(Ra cosϑ) was found to be in relationship according to power law. Hence, the logarithmic form of Eq. 4.10 can be linearly shown in the form:

$$ln(Nu) = A_o[ln(Ra\,cos\theta)]^p \tag{4.11}$$

Above relation has been obtained using relevant data points of concave curved flow duct passage, fitted with R-square method as shown in Fig. 4.14.

To get the power law relation between ln(A_o) with respect to ln(ϕ) trend can be written as follows. The variation trend observed in plot has been obtained using all the data point is shown in Fig. 4.15 and the equation obtained as;

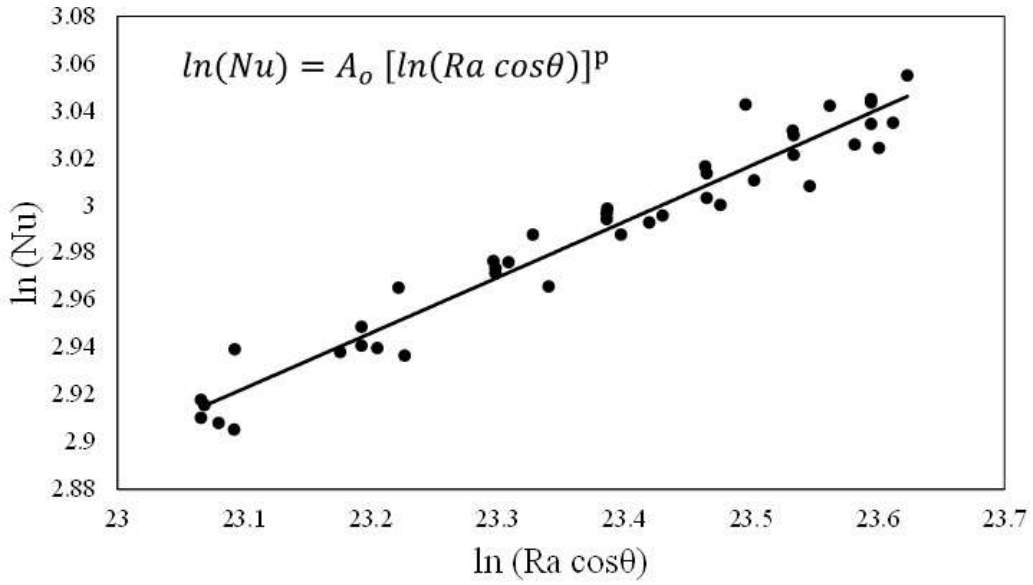

Figure 4.14: Plot of ln (Nu) versus ln (Ra cosϑ) of concave curved natural convective SAH.

$$A_o = B_o(\phi) \tag{4.12}$$

where coefficient $B_o = \left[\frac{Nu}{((Ra\,cos\theta)^p(\phi)^n)}\right]$ is a function of Nu, Ra andϕ.

The final correlation for Nusselt number is shown below;

$$lnNu = C_o[ln(Racos\theta)]^p(ln\phi)^n \tag{4.13}$$

where $C_o = 0.0089$,$n = 0.003$, and $p = 1.847$. Note that the correlation is valid for $\theta = 45°$, which is constant in our study.

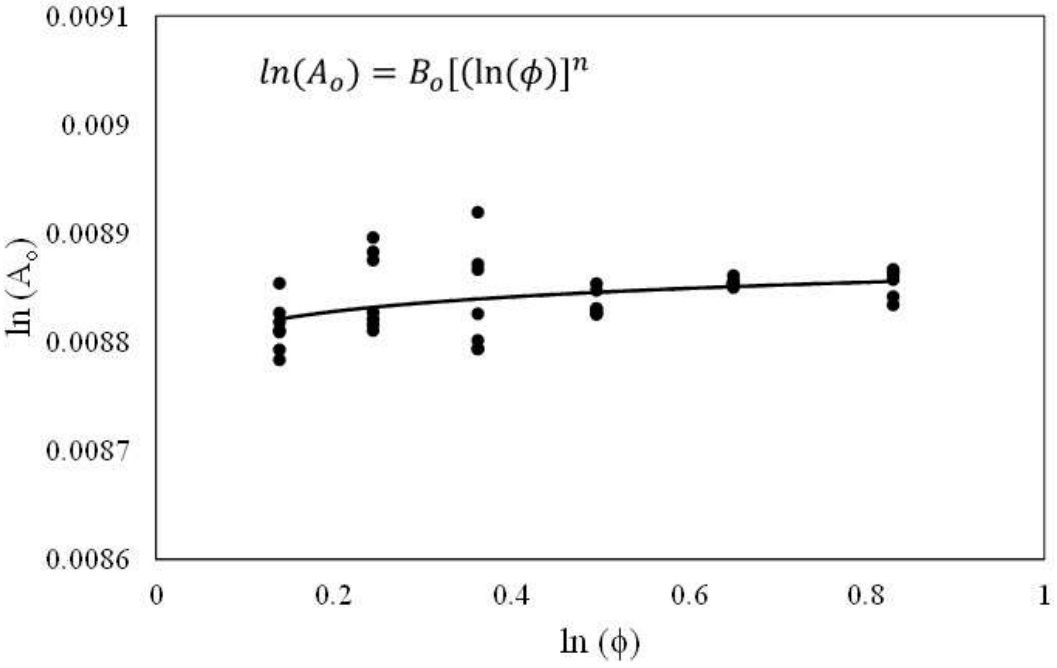

Figure 4.15: Variation of ln(A_o) versus ln(ϕ) of concave curved natural convective SAH.

4.5.2 Correlation development for convex curved design

Using the same methodology as above, the final correlation of Nusselt number for convex natural convective SAH is obtained and has the following form:

$$lnNu = C_1[ln(Ra\,cos\theta)]^r(ln\phi)^s \tag{4.14}$$

where $C_1 = 0.0047$, $s = 0.006$, and $r = 2.0507$;

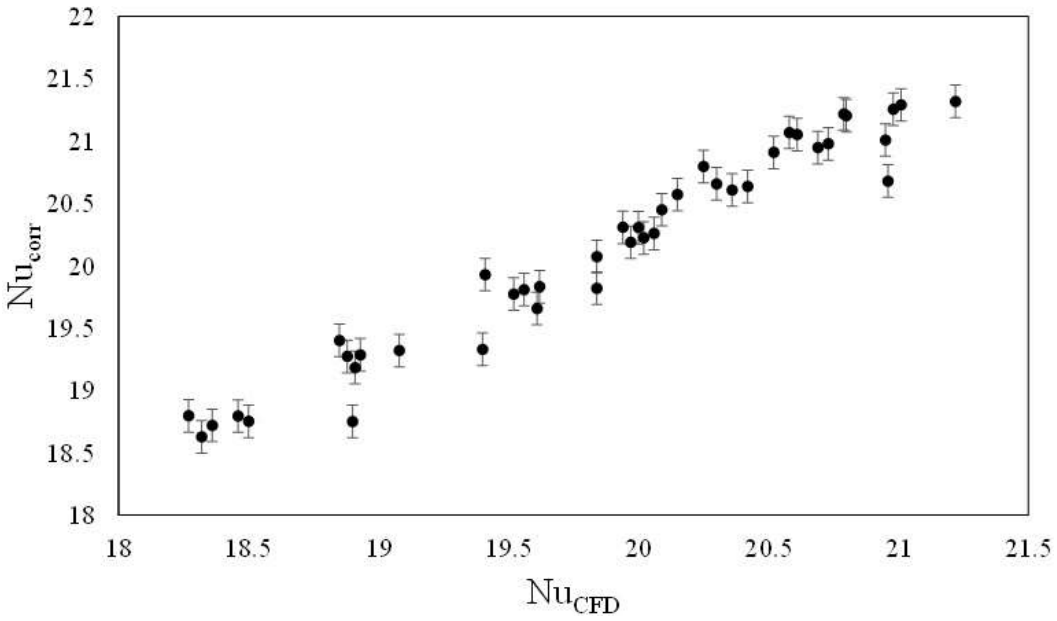

Figure 4.16: Comparison between values of Nusselt number correlation (Nu_{corr}) and Nusselt number CFD (Nu_{CFD}) of concave curved natural convective SAH.

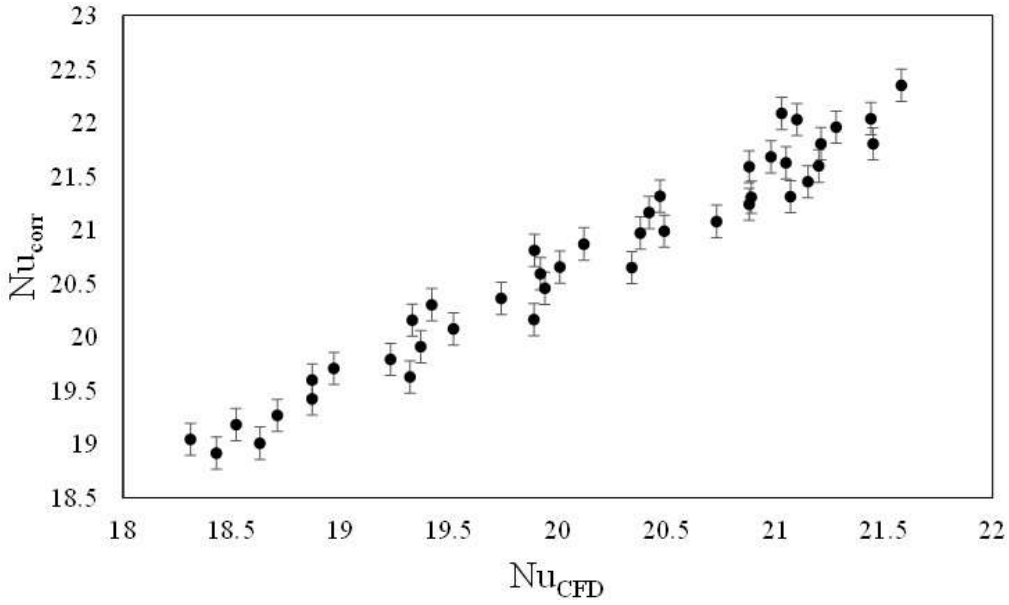

Figure 4.17: Comparison between values of Nusselt number correlation (Nu_{corr}) and Nusselt number CFD (Nu_{CFD}) of convex curved natural convective SAH.

4.5.3 Percentage error

The correlations for concave and convex design of natural convention SAH have been shown in the subsection 5.1 and 5.2, respectively. The set of all data points have been compared with the numerical results. Percentage error range incurred for the correlations of Nusselt number are shown in the Figs. 4.16 and 4.17.

Figures 4.16 and 4.17 shows the error in the values of Nusselt number associated with the concave and convex designs of SAH, when correlation data compared with the numerical results. The mean percentage error associated with concave designs were found to be 1.37%, respectively, while it is 2.95% in case of convex design of SAH.

4.6 Conclusion

Investigations on new designs of natural convection solar air heater has been done numerically for thermo-hydraulic performance improvement over convectional flat plate solar air heater. The two promising designs were studied: concave and convex for different range of curvature angle. The main purpose of the study was to enhance the thermal performance without significantly compromising on the hydraulic performance. The proposed concept designs are novel for SAH in natural convection scenario combined with chimney effect. Based on the outcomes of the investigations, some important conclusions have been drawn as mentioned below:

1. Thermo-hydraulic performance of the conventional flat plate solar air heater can be increased without incorporating any extended surfaces if flat parallel plate is transformed into concave and convex designs.

2. The convex and concave designs are 43% and 31%, respectively, thermally more effective than conventional flat natural convection SAH.

3. Nusselt number per unit pressure drop (Nu/P) was found to maximum for convex design. The average Nu/P values for convex and concave designs are respectively 7% and 6% higher than conventional flat parallel plate design for a constant heat flux condition.

4. Two new correlations were developed for Nusselt number as a function of Rayleigh numbers and curvature angle. These correlations were found to be in good agreement with the values of Nusselt number obtained numerically. The mean percentage error associated with concave designs were found to be 1.37%, respectively, while it is 2.95% in case of convex design of SAH.

We hope that these new designs and correlations would be helpful to scientist and industries in further development of thermally efficient designs of natural convection solar air heaters.